Dielectric Enhancement from Non-Insulating Particles with Ideally Polarized Interfaces and Zero ζ-Potential I: Exact Solution

Jiang Qian[1] and Pabitra N Sen[2]

[1] *4097 Silsby Road, University Heights, OH 44118*

[2] *35 Hazel Road, Berkeley, Ca 94705*

(Dated: October 25, 2016)

arXiv:1605.05029v2 [physics.class-ph] 23 Oct 2016

Abstract

We solve exactly the dielectric response of a *non-insulating* sphere of radius a suspended in symmetric, univalent electrolyte solution, with *ideally-polarizable* interface but *without* significant ζ-potential. We then use this solution to derive the dielectric response of a dilute random suspension of such spheres, with volume fraction $f \ll 1$, within the Maxwell-Garnett Effective Medium Approximation. Surprisingly, we discover a huge dielectric enhancement in this bare essential model of dielectric responses of solids in electrolyte solution: at low frequency $\omega\tau_D \ll (\lambda/a)/(\sigma_w/\sigma_s + 1/2)$, the real part of the effective dielectric constant of the mixture is $1 - (3f/2) + (9f/4)(a/\lambda)$. Here $\sigma_{w/s}$ is the conductivity of the electrolyte solution/solids, λ is the Debye screening length in the solution, $\tau_D = \lambda^2/D$ is the standard time scale of diffusion and D is the ion diffusion coefficient. As λ is of the order nm even for dilute electrolyte solution, even for sub-mm spheres and low volume fraction $f = 0.05$ the huge geometric factor a/λ implies an over 10^4-fold enhancement. Furthermore, we show that this enhancement produces a significant low frequency ($\omega\tau_D \ll 1$) phase shift $\tan\theta = \text{Re } \epsilon(\omega)/\text{Im } \epsilon(\omega)$ in a simple impedance measurement of the mixture, which is usually negligible in pure electrolyte solution. The phase shift has a *scale-invariant* maximum $\tan\theta_{\max} = (9/4)f/(2\sigma_w/\sigma_s + 1)$ at $\omega_{\max} = (2D/\lambda a)/(2\sigma_w/\sigma_s + 1)$. We provide a physical picture of the enhancement from an accumulation of charges in a thin Externally Induced Double Layer (EIDL) due to the blocking boundary condition on interfaces. This mechanism is distinct from the traditional dielectric enhancement in *insulating* particles due to large intrinsic ζ-potentials and surface charges, which predicts a different scaling for maximum phase shift frequency $\omega_{\max} = D/a^2$. Our model is also more transparent than that of Wong (*Geophysics* 44, 1245), which invokes different types of ions with or without Faradaic currents that obscure the physics behind his results. Finally we discuss data from geological samples containing sulfides and recent experiments on coke freeze that comport well with our predictions.

I. INTRODUCTION

In this paper we show, using an *exactly solvable model*, that a dilute suspension in electrolyte solution of non-insulating solid spheres with ideally polarized interfaces, across which no charge, electronic or ionic, is transferred between the solution and the solid, can give rise to huge dielectric constants (10^{5-6} or more) at low frequencies (KHz, far below plasma frequencies). This is remarkable considering that the electrolyte static permittivity is only about 80 while particle permittivity (due to core electrons and lattice) is about 1-5 at such frequencies. The only similar prior result we are aware of is by Wong [2], who used a fixed (zero) potential interface, which generally means an ideally *non*-polarizable interface [3] held at a constant potential by the redox reactions. But more important, Wong's analysis involved a medley of different kinds of ions, some with Faradaic (redox) reactions at the interface and other without. This made the physics obscure and source of the enhancement in his model is not clear. Here we strip down to essential physics and use an exactly solved model, derived from first principle, for *ideally polarizable interface* to show that dielectric enhancements are natural outcome in non-insulating particles in electrolyte solution, explicable without resorting to complex surface chemistry.

The enhancement here are produced on interfaces with zero ζ-potential. The dielectric enhancements with *insulating* clay-like charged particles with finite ζ-potentials suspended in electrolytes are well known [4–8], and are due to the Guoy-Chapman layer of the counter ions. Briefly, dry clay has a dielectric constant of about 5 and that of water is about 80 but the real part the dielectric in a clay - brine mixture can be as large as $\sim 10^4$ at low frequencies [4–11]. Standard Maxwell-Wagner / Maxwell-Garnett ([12–15]) analysis for a two-phase material is unable to explain such enhancements, see the Appendix I. Hinch *et. al.* [7] have nicely summarized the criticisms of previous ad hoc models [9] that "explained" the enhancement by endowing the particles with capacitative layers or layers with complex conductivity that could not be calculated from the first principles.

This clay-effect for insulating particles disappears when the ζ-potential is zero. Here we show that even with zero ζ-potential, non-insulating materials are capable of showing an dielectric enhancement, due to an Electrically Induced Double Layer (EIDL) produced by the low-frequency charge build-up from the blocking boundaries.

Analysis of electro-capillarity, electrophoresis and electro viscous forces on ideally polar-

izable metal drops require computing the polarizability of metallic spheres as we do–see the book by Levich [23] and references therein, and more recent papers [16–18].The term EIDL has been used by Bazant and his co-workers [16] in their study of electrokinetic effects. However these works do not consider the dielectric enhancement. Also, the previous work restrict themselves to the case of infinite particle conductivity, *i.e.*, an ideally polarizable surface that is an equipotential, with infinite conductivity for the metal particle. In our case we tackle solids of all conductivities, and indeed, we show below that the characteristic frequency for the enhancement depends on the ratio of the electrical conductivity of the particle and that of the electrolyte. We have used Levich's insight [23] to estimate the effect of electrokinetic flow on surface physics. In Ref. ([1]) we show that the electrophoresis does not affect the physics in the case of negligible ζ-potential. By contrast, for the finite zeta potential in clay like particles, the electrokinetic effect can be large–see, for example, Hinch *et. al.* [7] or Fixman[5]. We will thus not consider the electrokinetic effects here.

Electrochemistry touches many area of science and technology, ranging from biology, energy conversion, hydrolysis, batteries, corrosion in ships, bio-implants, pipeline corrosion, to geophysical explorations for minerals and hydrocarbon. One of the paradigm of interface is an ideally polarizable interface, the other being an ideally non-polarizable interface. The gap in the literature in understanding the enhancement in dielectric for the ideally polarizable non-insulating materials is glaring, because the interfacial processes at the solid-fluid interface have fundamental implications in the basic science of electrochemistry.

Noble metals, a common type of ideally-polarizable materials, are often used as contrast agent and markers in medicine. The optical properties of gold colloids are often exploited in the laboratory for markers in cancer cells. The possibility of using low frequency electrical property predicted here, where the depth of penetration is large, could be useful in clinical settings not unlike Electroencephalography imaging or impedance tomography[19] as in geophysical prospecting[2, 20–22, 25].

In geophysics deep-look using electromagnetic methods is of paramount interest[2, 20–22, 25]. First, the so-called Induced Polarization (IP) or high dielectric constant due to metallic deposits are routinely used in mineral exploration for gold and copper. See, for example, references in Seigel [25] and Wong [2]. Seigel *et. al.* [22, 25] trace the early development of the induced polarization method, starting with field observations by Conrad Schlumberger in a mining region in France in 1913. The enhanced dielectric constant has

been seen in numerous samples containing pyrite, chalcopyrite *etc.* [2, 20–22, 25], and more recently on graphitic materials like coke-breeze[20].

The second application is locating kerogeneous (source rock) material in shale gas and shale oil exploration[21] via the elctromagnetic response of pyrite nougats that often accompany the source. In the absence of a basic understanding of IP, people resort to ad hoc fitting routines like Cole-Cole plot [2, 22]. This work shows that the IP effect can be understood using fundamental physics. It may be possible to estimate the volume fraction as well as the size of the metallic nougats. These size and volume fraction parameters, in turn, contain valuable information of the geologic processes, such as the degree of maturity and the reducing nature of the depositional environment. Such information is useful for evaluation of the reservoir potential.

The third example entails using metallic grains as contrast agent in mapping fractures using dielectric tomography [20]. Hydraulic fractures in a gas or an oil well are induced to enhance flow and are kept opened by adding sand (proppant materials) to the hydraulic fluids. Most of the fractures close upon the removal of the applied hydraulic pressure. The fractures that remain open are the conduits of the hydrocarbon and hence mapping them is highly desirable. It has been proposed that by adding conducting material with high IP ("contrast agents") to sand one can map the zone using various geophysical electrical methods[21].

In this paper we study the exactly solvable case of spherical particles. In Ref.[1] we show that the dielectric enhancement observed in this paper is universal: it holds for non-insulating particles of arbitrary shape suspended in an electrolyte solution with ideally polarizable interfaces with small ζ-potential. Crucial for our results are the ideally-polarizable interface that "blocks" any dc (Faradaic) current. Our boundary conditions are different from that used previously, in that, we do not use a constant (zero-) potential boundary condition, but instead, apply the continuity of potential and the continuity of the normal component of the total current that comprises of the sum of displacement and conduction current. As the ions do not penetrate the solid, the current outside the solid is just the displacement current. Inside the solid it is a sum of the displacement current and the conduction current. In the hindsight the continuity of current seems obvious, but it has not been invoked previously in these problems. We show below these boundary conditions are crucial for the dielectric enhancement effect.

This paper is organized as following. In Sec. II we derive from the first principle our model of solids in electrolyte solution, explaining the approximation involved and their justifications and paying special attention to the critical boundary conditions used. Next, in Sec. III we solve exactly our model for a single sphere in solution, deriving the "Debye-like" form of the dielectric response. Building on this, in Sec. IV we compute the effective complex dielectric constant for a random mixture of spheres and electrolyte solutions from the Maxwell-Garnett theory of Effective Medium Approximation. We show that it exhibits a "Debye" form and at low frequency shows a huge enhancement of the real dielectric constant. Then in Sec. V we show that this enhancement renders the previously negligible phase shift (or loss-angle) in a simple impedance measurement observable. Indeed, we show that the phase shift has a maximum at the frequency $\omega_{\max} \approx 2D/(\lambda a)$ and not at $\omega_{clay} \approx 2D/a^2$ as in clay-like particles with finite zeta-potential [4–8]. For most materials, the height of the phase shift maximum $9f/4$ is scale-invariant and determined solely by the volume fraction. In Sec. VI we use an "effective boundary conditions", derived from a picture of EIDL, to link the physics behind the enhancement to the ideally-polarized blocking boundary conditions in Sec. II. Finally, in Sec. VII we discuss features of our predictions that have been seen in geological samples containing pyrite, chalcopyrite etc.[2, 22], and more recently on graphitic materials like coke-breeze[20].

II. GOVERNING EQUATIONS AND IDEALLY POLARIZED BOUNDARY CONDITIONS

Consider dielectrically uniform solid bodies immersed in an electrolyte solution. A uniform external field $E_0 \exp(i\omega t)$ drives the charge dynamics of the system. To emphasize physics and simplify notations, we assume the electrolyte solution contains a single species of cations and anions, with charges $\pm e$, and that they share the same diffusion coefficient D. Elsewhere [1], we show that our results can be easily generalized to the cases of asymmetric ions, as long as the fluid is charge-neutral when $E_0 = 0$.

The physics inside the simple, uniform dielectric solid is entirely characterized by a potential ψ_S, obeying Laplace's equation $\nabla^2 \psi_S = 0$. The physics in the electrolyte solution is characterized by more complex non-uniform charge dynamics. The potential in the liquid ψ

obeys Poisson equation:

$$\nabla^2\psi(\vec{r},t) = -\frac{\rho(\vec{r},t)}{\epsilon'_w\epsilon_0}; \qquad \rho(\vec{r},t) = e(N_+(\vec{r},t) - N_-(\vec{r},t)), \tag{1}$$

where ϵ'_w is the static dielectric constant for water and $N_\pm$ are the ion densities.

The motion of ions in the liquid is characterized by the current densities $\vec{j}^{\pm}_N$, which consist of three components: the diffusive current driven by ion density gradients, the conductive current driven by the electric field and a hydrodynamic current from ions being carried by the macroscopic motion of the liquid itself. Without significant ζ-potential and surface charge on solids, the net charge density in the solution is due entirely to the external field. The electrokinetic flow is governed by the Helmholtz-Smoluchowski equation [23], and is proportional to E_0^2. Elsewhere [1], we show that the ionic currents carried by such an electrokinetic flows are much smaller than the conductive currents, which is proportional to E_0, and can be safely ignored in the low-frequency and low-field linear limit discussed in this paper.

So the ionic currents $\vec{j}^{N}_{\pm}$ in the solution consist of a diffusive and a conductive part, related to each other by the Einstein relation. These currents also determine the dynamics of ion densities through number conservation laws:

$$\vec{j}^{N}_{\pm} = -D\left(\vec{\nabla}N_\pm \pm \frac{eN_\pm}{k_BT}\vec{\nabla}\psi\right), \quad \vec{\nabla}\cdot\vec{j}^{N}_{\pm}(\vec{r},t) = -\frac{\partial N_\pm(\vec{r},t)}{\partial t} \tag{2}$$

Eq. 1 and Eq. 2 fully characterize the physics in the electrolyte solution with a set of coupled non-linear partial differential equations. Major further simplifications come from the assumptions that both the ζ-potential and the driving field are small: $e\psi_\zeta \ll k_BT$, $eE_0a \ll k_BT$, where a is the maximum linear dimension of the solids in the direction of the $\vec{E}_0$. Under these conditions, we have shown elsewhere [1] that, when the ion densities are divided into a background density $N^0_\pm = N$ in the absence of the external drive E_0 and a perturbation due to the E_0, $N_\pm = N + n_\pm$, the background is nearly uniform $\vec{\nabla}N \approx 0$ and the perturbations are small $n_\pm \ll N$. With these assumptions, the governing equations for the physics in the liquid linearize:

$$\vec{\nabla}\cdot\vec{j}_\pm = i\omega n_\pm, \quad \vec{j}_\pm = -D\left(\vec{\nabla}n_\pm \pm \frac{eN}{k_BT}\vec{\nabla}\psi\right), \quad \nabla^2\psi = -\frac{e(n_+ - n_-)}{\epsilon_0\epsilon'_w}. \tag{3}$$

To implement the ideally polarized boundary conditions (BCs), we note that the ions cannot penetrate the solid, and at the same time the solid is not a source of ions. Furthermore, electrons do not transfer across the interfaces [2, 3]. In this case, no charge transfer

between the solids and the electrolyte solution occurs at the interface, the interfaces are called "perfectly polarizable" or "ideally polarizable". The text-book example of an "ideally polarizable" interface is a platinum electrode. For ideally non-polarizable interface, such as silver/silver chloride system in a brine, chlorine reacts with silver/silver chloride electrode, and a Faradaic current can freely pass (without polarization) through the interface. The difference between ideally polarized and non-polarizable surfaces has been explained exceedingly well by Wong [2]. The ideally polarized boundary condition means the normal components of ionic currents must vanish at solid-liquid surfaces:

$$\widehat{u}\cdot j_{\pm}|_{\mathbf{\Sigma}}=0\ \ [\mathbf{a}],\quad \psi_S=\psi\ \ [\mathbf{b}],\quad (\sigma_s+i\omega\epsilon_0\epsilon'_s)\widehat{u}\cdot\overrightarrow{\nabla}\psi_S=(i\omega\epsilon'_w\epsilon_0)\,\widehat{u}\cdot\overrightarrow{\nabla}\psi\ \ [\mathbf{c}] \tag{4}$$

Here $\mathbf{\Sigma}$ are the liquid-solid interfaces and $\hat{u}$ is the normal vector on $\mathbf{\Sigma}$. ϵ'_s, σ_s are the *static* dielectric constant and conductivity of solid bodies. We assume in this paper the frequency is much below the plasma frequencies of either the liquid or the solids, so that the real dielectric constants and conductivities can be considered frequency-independent. The conditions [**b**] [**c**] are just the standard BCs for potentials across dielectric interfaces. In particular, [**c**] is derived, as usual, from the conservation of currents across the interfaces Σ, with the special requirement that the ionic currents on the liquid side are zero due to condition [**a**], so there are only displacement currents on the liquid side.

The symmetry between cations and anions, though not essential to our conclusions, does afford a further simplification of our formalism. Introduce the total net ionic density $n^{\text{total}} = n_+ + n_-$ and the net density $n^{\text{net}} = n_- + n_-$. It is easy to transform the equations of motion Eq. 3 and the BCs Eq. 4 to *decoupled* equations for n^{total} and n^{net}. Furthermore, because the equation of motions and BCs for n^{total} are entirely decoupled from the potential ψ, it is easy to show $n^{\text{total}}(\vec{r},t)=0$ throughout the liquid and at all time.

Only n^{net} is coupled to ψ and has non-trivial dynamics. Combining the charge conservation and Poisson's Equation in Eq. 3, the equations of motion take a very simple form:

$$\nabla^2 n^{\text{net}}=\beta^2 n^{\text{net}};\qquad \nabla^2\psi=-\frac{en^{\text{net}}}{\epsilon_0\epsilon'_w};\quad \beta^2\lambda^2=1+i\,\omega\tau_D;\quad \tau_D=\frac{\lambda^2}{D}=\frac{\epsilon_0\epsilon'_w}{\sigma_w}. \tag{5}$$

Here we introduce the characteristic time scale of the charge dynamics in the liquid τ_D, which typically ranges from 10^{-10}s to 10^{-7}s from concentrated to dilute electrolyte solution, and the Debye length λ, which ranges from 0.3nm to 10nm. In this paper, we always consider low frequency $\omega\tau_D \ll 1$, so $\beta \approx 1/\lambda$. Finally, the boundary conditions can also be significantly

simplified:

$$\hat{u}\cdot\vec{\nabla}n^{\rm net}+\frac{1}{\lambda^2}\frac{\epsilon_0\epsilon'_w}{e}\hat{u}\cdot\vec{\nabla}\psi=0.\ [\mathbf{a}],\quad \psi_S=\psi\ [\mathbf{b}],\quad \hat{u}\cdot\vec{\overrightarrow{\nabla}}\psi_S=c\,\hat{u}\cdot\vec{\overrightarrow{\nabla}}\psi\ [\mathbf{c}]. \tag{6}$$

Here we introduced constant c to simplify notations and used the following form of λ, derivable from the Einstein relations:

$$c=\frac{i\omega\epsilon'_w\epsilon_0}{\sigma_s+i\omega\epsilon_0\epsilon'_s},\qquad \lambda^2=\frac{k_BT\,\epsilon_0\epsilon'_w}{2Ne^2}. \tag{7}$$

III. DIELECTRIC RESPONSE OF A SINGLE SPHERE IN AN ELECTROLYTE SOLUTION

For a single solid sphere of radius a in an electrolyte liquid, the solution of the Laplace equation for ψ_S in the solid and the pair of equations 5 for $n^{\rm net}$ and ψ in the liquid, coupled under BCs Eq. 6, is straightforward. The general solutions for the homogeneous equations of ψ_S (Laplace, finite at the origin) and of $n^{\rm net}$ (Helmholtz, finite at infinity) are well-known:

$$\psi_S(r,\theta)=\sum_l A_l\ P_l(\cos\theta)\ r^l,\qquad n^{\rm net}(r,\theta)=\sum_l B_l\ P_l(\cos\theta)\ k_l(\beta r), \tag{8}$$

where P_l are Legendre polynomials and k_l are modified spherical Bessel functions of the second kind. The inhomogeneous Poisson equation for ψ has an obvious special solution due to its structural similarity to the Helmholtz equation for $n^{\rm net}$: $\psi^{\rm special}=-(1/\beta^2)(e/\epsilon_0\epsilon'_w)n^{\rm net}$. The general solution for the homogeneous Laplace equation, for which $\psi^{\rm hom}$ becomes the driving potential $-E_0r\cos(\theta)$ for $r\gg a$, is simply $-E_0rP_1(\cos\theta)+\sum C_lP_l(\cos\theta)r^{-l-1}$. Thus, the general solution for potential ψ in the liquid is:

$$\psi(r,\theta)=-E_0rP_1(\cos\theta)+\sum_l P_l(\cos\theta)\left(C_l\ r^{-l-1}+\left(-\frac{e}{\epsilon_0\epsilon'_w}\frac{1}{\beta^2}\right)B_l\ k_l(\beta r)\right). \tag{9}$$

Combining Eq. 8 and Eq. 9 with BCs. Eq. 6, where the normal current is simply the radial derivative against r, it is easy to see that for any angular eigenvalue $l\neq 1$, because of the absence of external drive term E_0, the three BCs produce three homogeneous linear equations with a non-zero determinant and thus force $A_l=B_l=C_l=0$. The remaining three $l=1$ coefficients can be easily solved through matching BCs, giving an exact solution for the potential and charge distribution in the liquid and the sphere.

It is crucial to note that the simple grouping in Eq. 9 by their angular eigenvalues l depends crucially on that P_l are *shared* eigenfunctions for the angular part of axially-symmetric

Laplace and Helmholtz equation. The same trick does *not* work for even the slightly less symmetric geometry of a spheroid whose symmetry axis aligns with the direction of the driving field $\vec{E}_0$. For the spheroid geometry the coupled equations of the Laplace Equation for ψ_S and Eq. 5 under BCs Eq. 6 are *non-separable*.

The three terms of the potential ψ in the liquid has straightforward physical interpretations. $-E_0 r\cos\theta$ is the driving field. The term with modified spherical Bessel function $k_l(\beta r)$ decays exponentially from the interface $\mathbf{\Sigma}$ over the scale $|1/\beta| \approx \lambda \ll a$. The term $C_1\cos\theta/r^2$ are precisely that of an induced dipole. If we define a polarization P by the far field potential $\psi(|\vec{r}| \gg a) \to P\,a^3\,\vec{E}_0\cdot\vec{r}/(|\vec{r}|^3) - \vec{E}_0\cdot\vec{r}$, the exact solution above gives the following form of P:

$$P = 1 - \frac{3}{2 + [\epsilon_w(\omega)/\epsilon_s(\omega) + g/i\omega\tau_D]^{-1}},\ g = \left(a\beta + 1 + \frac{1}{a\beta+1}\right)^{-1},\ \epsilon_{w/s}(\omega) = \epsilon'_{w/s} + \frac{\sigma_{w/s}}{i\omega\epsilon_0}, \tag{10}$$

where the last equation is simply the standard form of the low-frequency complex dielectric constants for the liquid and the solid with the assumptions of frequency-independent ϵ', σ.

This exact solution for P can be simplified considerably under the low frequency regime in this paper. First, as noted below Eq. 5, we focus on $\omega\tau_D \ll 1$ so $\beta \approx 1/\lambda$. As λ is of the order 10nm even for dilute electrolyte solution, the radius of spheres $a \gg \lambda$ even for micron-sized microscopic particles, therefore $a\beta \approx a/\lambda \gg 1$, $g \approx \lambda/a$ in Eq. 10 above. Furthermore, we can rewrite the ratio between complex dielectric constants as

$$\frac{\epsilon_w(\omega)}{\epsilon_s(\omega)} = \frac{\sigma_w}{\sigma_s}\frac{1+i\omega\tau_D}{1+i\omega\tau_S} \approx \frac{\sigma_w}{\sigma_s},\quad \omega\tau_D \ll 1,\quad \omega\tau_S = \omega\tau_D\frac{\epsilon_s}{\epsilon_w}\frac{\sigma_w}{\sigma_s} \ll 1. \tag{11}$$

Here the definition of τ_S for the solid is completely analogous to that of τ_D in Eq. 5. As ϵ'_s/ϵ'_w is generally between 0.01 and 0.1, as long as the solid is *non-insulating*, the second condition above is not much more stringent than $\omega\tau_D \ll 1$.

With these two approximations, the exact solution for P reduces to a "Debye-like" form:

$$P = P_0 + \frac{P_1}{1+i\omega\tau_C},\quad P_0 = 1 - \frac{3\ \sigma_w/\sigma_s}{1+2\ \sigma_w/\sigma_s},\quad P_1 + P_0 = -\frac{1}{2},\quad \tau_C = \tau_D\ \frac{a}{\lambda}\left(\frac{\sigma_w}{\sigma_s} + \frac{1}{2}\right). \tag{12}$$

As we shall see below, the new time scale τ_C, geometrically enhanced by a huge factor a/λ profoundly alters the physics and gives rise to the dielectric enhancement.

IV. DIELECTRIC RESPONSE FOR A RANDOM SUSPENSION OF SPHERES IN AN ELECTROLYTE LIQUID

We now proceed to evaluate the linear response of a dilute suspension of spheres in Sec. III, with a volume fraction $f \ll 1$, in the electrolyte solution. For this we employ the Maxwell [12] or the Maxwell-Garnett [13–15] effective medium approximation. In this theory, the effective complex dielectric constant $\epsilon_{\text{eff}}(\omega)$ obeys the Clausius-Mossotti Relation [14, 15]:

$$fP = \frac{\epsilon_{\text{eff}}/\epsilon_w(\omega) - 1}{\epsilon_{\text{eff}}/\epsilon_w(\omega) + 2}, \quad \frac{\epsilon_{\text{eff}}}{\epsilon_w(\omega)} \approx 1 + 3fP, \quad \frac{\epsilon_{\text{eff}}}{\epsilon'_w} = \left(1 + \frac{1}{i\omega\tau_D}\right)(1 + 3fP) \approx \frac{1}{i\omega\tau_D}(1 + 3fP). \tag{13}$$

In the first step we use the fact that when $f \ll 1$, $|fP| \ll 1$, which is easy to verify with Eq. 12. The next step we simply use the fact that at low frequency $\omega\tau_D \ll 1$, $\epsilon_w(\omega)$ is dominated by its imaginary parts from conduction.

Putting Eq. 12 and Eq. 13 together, we obtain the following Debye form of effective dielectric constant for a dilute $f \ll 1$ suspension of non-insulating spheres under the two low-frequency conditions Eq. 11:

$$\frac{\epsilon_{\text{eff}}}{\epsilon'_w} \approx \left(1 - \frac{3}{2}f\right)\frac{1}{i\omega\tau_D} + \frac{9f}{4}\frac{a}{\lambda}\frac{1}{1 + i\omega\tau_C}. \tag{14}$$

The first term in ϵ_{eff} is simply the divergent imaginary part of $\epsilon_w(\omega) = \epsilon'_w + \sigma_w/(i\omega\epsilon_0) = \epsilon'_w[1 + 1/(\omega\tau_D)]$ of the electrolyte solution, now slightly modified by the dilute suspension (the $3f/2$ term). This terms is purely imaginary, so $\text{Re}(\epsilon_{\text{eff}}(\omega)$ is entirely determined by the second term.

That second term is rather more consequential. At low frequency, it produces a large, material-independent enhancement to the static dielectric constant:

$$\text{Re}(\epsilon_{\text{eff}}(\omega)) = \left[\left(1 - \frac{3}{2}f\right) + \frac{9}{4}\frac{a}{\lambda}f\right]\epsilon'_w, \quad \omega\tau_C \ll 1, \ \ or \ \ \omega\tau_D \ll \frac{\lambda}{a}\frac{1}{\sigma_w/\sigma_s + 1/2}. \tag{15}$$

Here we have included, for completeness's sake, insignificant contributions $(1 - 3f/2)$ from the terms neglected in the last step of Eq. 13. The enhancement, scaling with a/λ and independent of the material properties, such as ϵ_s and σ_s of the solids, is determined solely by geometry. The condition for observing the enhancement is governed not by τ_D, but by a new time scale dependent on both the geometry and the conductivity of the solid spheres.

We will discuss the physical origin of this time scale in more details below. Here we only note that, the larger is the geometric enhancement factor a/λ, the correspondingly lower

one has to go to observe the enhancement. Furthermore, if the solid is insulating $\sigma_s \to 0$, the condition in Eq. 15 can never be satisfied and there is no dielectric enhancement.

V. SCALE-INVARIANT MAXIMUM OF PHASE SHIFT

In general the dielectric measurements at low-frequencies are exceedingly difficult[33], precisely because the imaginary contributions from conduction dominates over the real part of the dielectric constant. The large enhancement predicted in the last section, however, should make this observation easier. To show this, let us compute the phase shift in complex dielectric constant, defined as $\tan\theta = \arg\epsilon_{\text{eff}}(\omega) = \text{Re}(\epsilon_{\text{eff}})/\text{Im}(\epsilon_{\text{eff}})$, which is easily observable in simple impedance measurements.

For pure electrolyte solution without the solids, the phase shift is at low frequency is simply $\omega\tau_D$. As τ_D is $10^{-7}s$ even for a very dilute electrolyte solution, and $\omega\tau_D \ll 1$, the phase shift is about 0.1 miliradians for frequencies at kHz range. The dielectric enhancement of $(9f/4)(a/\lambda)$ boost this low frequency phase shifts by orders of magnitude with the introduction of an even dilute suspension of spheres, making it much more observable.

More quantitatively, let us rewrite Eq. 14 to this more convenient form:

$$\begin{aligned}\frac{\epsilon_{\text{eff}}}{\epsilon'_w} &\approx \frac{a}{\lambda}\left(\sigma_w/\sigma_s + \frac{1}{2}\right)\left[\left(1 - \frac{3f}{2}\right)\frac{1}{i\omega\tau_C} + \frac{9f}{4\sigma_w/\sigma_s + 2}\frac{1}{1 + i\omega\tau_C}\right] \\ &\approx \frac{a}{\lambda}\left(\sigma_w/\sigma_s + \frac{1}{2}\right)\left[\frac{1}{i\omega\tau_C} + \frac{9f}{4\sigma_w/\sigma_s + 2}\frac{1}{1 + (\omega\tau_C)^2}\right] \end{aligned} \tag{16}$$

The second step relies on the fact that $f \ll 1$, so both the $-3f/2(1/i\omega\tau_D)$ contribution and the imaginary part of the Debye term are small compared with $1/(i\omega\tau_D)$. Now it is trivial to see that the phase shift and its maximum are:

$$\tan\,\theta(\omega) = \frac{9f}{4\sigma_w/\sigma_s + 2}\frac{\omega\tau_C}{1 + (\omega\tau_C)^2}, \qquad \tan\,\theta(\omega_{\max}) = \frac{9f}{4}\frac{1}{2\sigma_w/\sigma_s + 1}. \tag{17}$$

The maximum of phase shift is observed at frequency $\omega_{\max}\tau_C = 1$, or spelling out the geometric and material dependence explicitly:

$$\omega_{\max}\tau_D = \frac{2\lambda}{a}\frac{1}{1 + 2\sigma_w/\sigma_s}, \;\; or \;\; \omega_{\max} = \frac{2D}{\lambda a}\frac{1}{1 + 2\sigma_w/\sigma_s}. \tag{18}$$

Two features stands out from these results. The maximum phase shift is *scale-invariant*. Indeed, given that even strong electrolyte solutions like the sea water and the human blood

has conductivity σ_w of the order S/m, and even moderately doped semiconductor has σ_s orders of magnitudes higher, it is very often safe to assume $\sigma_s \gg \sigma_w$ for non-insulating solids. In such a case, the maximum phase shift depends *solely* on volume faction f and is very significant: even for a small volume faction $f = 0.05$, θ reaches over 100 miliradian. Dielectric enhancement from even a dilute suspension of non-insulating spheres boosts the minuscule phase shift of an electrolyte solution to an easily observable level.

The second feature is that the frequency $\omega_{\max}$ at which the maximum above is observed is inversely proportional to the size of the spheres. This is different from the scaling of the maximum frequency of phase shift observed in clay particles $\omega_{\max} = D/a^2$ [4–7]. The mechanism for dielectric enhancement in that case, the large ζ-potentials and surface charges, is entirely different from ours.

VI. EFFECTIVE BOUNDARY CONDITIONS AND THE PHYSICAL PICTURE

From the Sec. III and Sec. IV above, we see that the origin of the dielectric enhancement is the small but non-vanishing imaginary part in the dielectric response of the sphere P that *persists at low frequency* $\omega\tau_D \ll 1$. That imaginary part, the $g/(i\omega\tau_D)$ in Eq. 10 which gives rise to the $i\omega\tau_C$ in Eq. 12, form a *cross term* that, when multiplied by the *diverging* imaginary conduction contribution from the electrolyte solution $1/(i\omega\tau_D)$ in Eq. 13, produces the large *real* dielectric constant at low frequency. As we show in Appendix I, without that term, at $\omega\tau_D \ll 1$ and $\omega\tau_S \ll 1$ (*c.f.* Eq. 11) P is purely real and there is no enhancement. So a physical picture of the enhancement need to account for this imaginary part.

From Eq. 8 and Eq. 9, it is easy to observe that, in the liquid, the net charge n^{net} decays exponentially over the distance of order λ, and the potential ψ, aside from the long range parts due to the external drive and the induced dipole, also does so. It is then natural to separate out the physics within these thin, charged layers within a few λ from the solid-liquid interfaces, which we call the "Exteranlly Induced Dipole Layers"(EIDL), from the *charge-neutral* homogeneous bulk liquid outside it. The potential ψ_L in the neutral bulk liquid, just like the potential within the solid ψ_S, follows the much simpler Laplace equation, and is thus a harmonic function.

By analyzing the charge dynamics and potential within the EIDL, we can derive effective

boundary conditions (BCs) connecting harmonic potentials ψ_S and ψ_L,:

$$\epsilon_s(\omega)E_S^\perp = \epsilon_w(\omega)E_L^\perp \quad [\mathbf{a}], \quad \psi_S = \psi_L + \frac{1}{i\omega\tau_D\beta}E_L^\perp. \quad [\mathbf{b}], \tag{19}$$

where $\epsilon_{w/s}(\omega)$ are defined in Eq. 10.

While detailed derivation of these BCs can be found in another publication [1], the basic idea is straightforward. It is easy to see from Eq. 8 and Eq. 9 that the spatial variation within the EIDL is much more rapid in the normal direction, where both n^{net} and ψ vary on the scale of λ, than in the tangential direction, where they vary on the scale of a. The governing equations Eq. 5 therefore reduce into 1D problems in the normal direction $\hat{u}$, and each spatial derivative simply contributes a factor of $-\beta$, just as each time derivative contributes a factor of $i\omega$ under a harmonic drive.

Furthermore, the normal net current $j^{\text{net}} = j^+ - j^-$ consists of a constant contribution from outside the EIDL $j^{\text{out}} = \sigma_w E_L^\perp$ ($E_L^\perp$ is the normal field in the charge neutral liquid *just outside* the EIDL) and a current j^{var} from within the EIDL that varies spatially as $\exp(-\beta z)$. Charge conservation $\partial n^{\text{net}}/\partial t + \vec{\nabla} j = 0$ then dictates $\beta j^{\text{var}} = i\omega n^{\text{net}}$ throughout the EIDL. Finally, the critical boundary condition that the normal current vanishes at the liquid-solid interface $j = j^{\text{var}} + j^{\text{out}} = 0$ (*c.f.* Eq. 4a) implies that the net particle density at that interface n_0 satisfies:

$$j^{\text{out}} = \sigma_w E_L^\perp, \quad \beta j^{\text{var}} = i\omega n^{\text{net}}, \quad j = j^{\text{var}} + j^{\text{out}} = 0, \quad n_0 = -\frac{E^\perp \beta \sigma_w}{i\omega e} \tag{20}$$

Since within the EIDL $n(z) = n_0 \exp(-\beta z)$, with one spatial integration of the Poisson equation one can find how the normal field $E^\perp$ varies across the EIDL, and with another integration one can obtain the potential drop across it.

The physical interpretation of the effective BCs Eq. 19 is straightforward. Recall that in Eq. 4 [**c**], the conduction current is missing at the boundary between the solid-liquid interfaces. Eq. 19 [**a**] shows that, after taking into account of the charge dynamics within the EIDL, the ordinary BC for harmonic potentials on conductive boundaries is restored between the harmonic potentials ψ_S and ψ_L on either side of the EIDL.

The second BC Eq. 19 [**b**] is more significant. The discontinuity between ψ_L and ψ_S comes from the dipole moment produced by a large, inhomogeneous charge build-up within the EIDL. This dipole moment is out of phase (purely imaginary) from the driving field, because the driving field is proportional to the j^{out} in the EIDL (Eq. 20), whereas the charge

dynamics is always within the EIDL is *always out of phase* from j^{var} (*ibid.*), and the two currents are linked by the perfectly polarizable boundary condition $j = 0$. As we will see below, it is precisely this out of phase dynamics that generates the imaginary part of P in Eq. 12 and thus produces the dielectric enhancement. Furthermore, as the driving frequency ω decreases, the charge dynamics slows and this forces a larger charge build up n_0 within one period $T = 2\pi/\omega$ in the EIDL (Eq. 20). Thus the induced dipole of the EIDL and the dielectric enhancement are inherently low-frequency phenomena.

Finally, the special symmetry of the sphere geometry permits a particularly simple solution from the effective BCs Eq. 19. As noted in Sec. III, due to the symmetry of the driving field, only terms with $P_1 = \cos\theta$ angular dependence survive in all potentials and densities. In particular, the electric field E_S within the solid sphere is uniform and parallel to the external drive. This means that, on the sphere surface, the normal electric field at polar coordinate (θ, ϕ) is simply $E_S \cos\theta$. Setting $\psi_S = 0$ at the origin, the potential at (θ, ϕ) is $-Ea\cos\theta$. Thus, for a sphere in a uniform driving field, $\psi_S/E_S^{\perp} = -a$, *throughout* the solid-liquid boundary $\mathbf{\Sigma}$. This allows us to convert the dipole term in Eq. 19 [**b**] back to ψ_S via Eq. 19 [**a**]. By rescaling rescaled internal potential and field with a proper factor to ψ_S' and E_S', we can transform the boundary conditions Eq. 19 into a "conventional" boundary value problem, without the dipole layer between two homogeneous medium, that leaves the potential outside ψ_L *unchanged*, only with a new relative permittivity:

$$\epsilon'(\omega)E_S'^{\perp} = \epsilon_w(\omega)E_L^{\perp}, \quad \psi_L' = \psi_L, \quad \frac{\epsilon_w(\omega)}{\epsilon'(\omega)} = \frac{\epsilon_w(\omega)}{\epsilon_s(\omega)} + \frac{\lambda}{a}\frac{1}{i\omega\tau_D}. \tag{21}$$

From elementary electrostatics we know that for a sphere with dielectric constant ϵ' immersed in an uniform medium with ϵ_w, the induced polarization, as defined above Eq. 10 $P = 1 - 3/(\epsilon'/\epsilon_w + 2)$. With the peculiar relatively permittivity in Eq. 21, this elementary result immediately leads to the exact solution Eq. 10. The sole difference is the reduction of g in Eq. 10 to λ/a, which is valid when $\omega\tau_D \ll 1$ and $\lambda \ll a$. These are precisely the conditions for effective BCs Eq. 19 in the EIDL approximation [1]. This solution also makes it clear that the origin of the imaginary term in P at low frequency $\omega\tau_D \ll 1$ is due solely to the imaginary dipole layer term in Eq. 19 [**b**].

VII. APPLICATION TO EXPERIMENTS

There are numerous experiments that show dielectric enhancement in metallic particles. IP is an important tool in prospecting for copper. Porphyry copper deposits, for example, contain disseminated conducting chalcocite (Cu_2S), chalcopyrite ($CuFeS_2$), and pyrite (FeS_2) embedded in a porous matrix that is predominantly feldspar, quartz, and mica. The conducting grains, in most types of mineral deposits, are in contact with brine that fills the pore space, and, produce huge IP signals in the field measurements. Hence there are quite a large number of laboratory data on these materials. Wong[2] cites data by numerous authors; see also the references cited in [22, 24] as well as those cited by Seigel et al.[25] in their review of the history of IP. In many ways these experiments are uncontrolled as many important parameters such as pH, reactions effects, if any, the ζ-potential were not measured separately. More relevant for our model of mono-sized spherical grains, The shapes and homogeneity of the particles are not guaranteed. Nelson and Van Voohris[22] emphasize that the deficiency in their data lies in the fact that the cation exchange capacity (CEC), that is directly related to the ζ-potential, were not measured.

Figure 14. in Ravel [22] shows a typical phase-shift and in-phase conductivity for Pyrite content of 1 percent in weight (10 mg/g) in sand or in agar gel. It has features that are not unlike the figure below, Fig(1). As mentioned above, the phase shift maximum varies inversely with the particle size[2, 24], for the smaller particles, and data agrees with Eq. (18). It can be surmised that these may be ideally polarizable samples. The data in the geophysical literature show dielectric enhancement in many metallic and semiconducting particles and the height in the phase shift maximum depends linearly on the volume concentratio[2, 22]. Preliminary experiments with conductive particles that have putatively zero zeta potential such as iron and carbonaceous particles("coke-breeze") [26] show the behavior predicted here–$\tan\theta$ depends linearly on the volume fraction f.

The maximum of $9f/4$ is easily observable by a commercial instrument, which often have 0.1-milirad sensitivity, even for a very small volume fraction f. When designing contrast agent, one is often restricted by various practicality, like the frequency used by the apparatus or the in-situ conductivity. The above two equations Eqs. *i.e.*, Eq. (17) and Eq.(18) will serve as a guide in designing the materials and their sizes.

The dielectric spectroscopy and the dielectric enhancement are important tools in biology

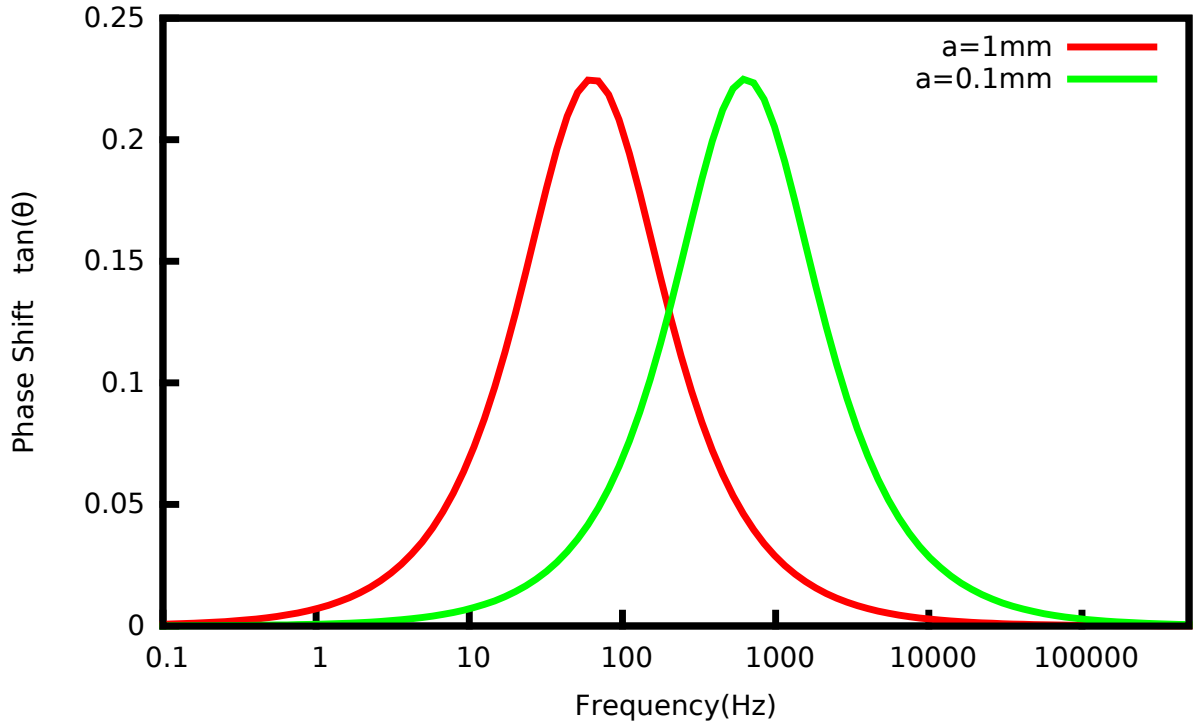

FIG. 1: A plot of $\tan\theta$ in Eq. (17), for volume fraction $f = 0.1$ and electrolyte concentration $10^{-3}M$, as a function of the frequency ω. Spheres of radius $a = 0.1mm, 1mm$ are plotted. It was assumed that the material conductivity is much greater than that of water. While the position of the maximum moves to higher frequencies, $\omega_{\max} = 2D/(\lambda a)$, for a smaller size, the height remains the same as seen in experiment by [26]. Also a linear dependence on volume fraction f is seen in the experimental data [22, 24–26].

[27, 28, 33]. Many complex macromolecules have fixed charges [27] and have Guoy-Chapman like double layer and the dielectric enhancement can be likened to those of clay [4–7]. The dielectric spectroscopy has been used widely in other biological systems like blood. However blood has strong ionic conductivity. The dielectric constant generally increases with lowering frequency from the dielectric of the host and ending with a plateau with the enhanced value. Blood shows rather complicated dielectric response[28] with two plateaus, as the frequency is lowered. It has been suggested that the plateau lower frequency enhancement is perhaps due to and "blocking" effect. This requires more careful examination as the membranes are not impermeable to ions. The above analysis needs to be be extended to incorporate both finite ζ-potential and finite permeability of the membrane.

Finally, we would like to draw attention of the reader to Ref.[1] where we show that the dielectric enhancement is nearly universal for ideally polarizable interfaces *i.e.* homogeneous particles of arbitrary shape suspended in an electrolyte solution. Furthermore, in this paper, to emphasize the physics and simplify notations, the solution contains only one species each of cations and anions, with equal and opposite charges and equal diffusion diffusion coefficients of the cations and anions are D_+, D_-. We show in [1] that asymmetric ions with distinct charges and diffusion coefficients have the same physics. We also show in [1] that the Electrophoretic Flow is insignificance in the present problem of dielectric enhancement.

VIII. ACKNOWLDGEMENTS

At the early stages of this work, one of us (Sen) was partially supported at the University of North Carolina, Chapel Hill, by the Advanced Energy Consortium: http://www.beg.utexas.edu/aec/ whose member companies include BP America Inc., Total, Shell, Petrobras, Statoil, Repsol, and Schlumberger. Sen is grateful to Alfred Kleinhammes for stimulating discussions and collaborations on experiments.

Appendix I: Absence of Dielectric Enhancement without Ionic Effects

In the text-book [12] examples of potential induced by a sphere with zero ζ-potential, the conductivity in the host is driven by the electrical potential gradient times σ_w and there are no currents from the gradients in the carrier densities. The potentials both inside and outside the sphere are governed by the Laplace's equation, i. e. the charge imbalance is zero in the Poisson's equation. In this case although there is an induced surface charge density on the surface of the sphere–there is no EIDL. We briefly recollect that without a double layer like EIDL or a Guoy-Chapman layer, there is no enhancement. For a sphere of dielectric ϵ_{in}, suspended in a continuum ϵ_w

$$P = \frac{\epsilon_{in} - \epsilon_w}{\epsilon + 2\epsilon_w}, \tag{22}$$

as given in [12].

For inclusions with non-zero conductivity $\epsilon_{in} = \epsilon'_{in} + \sigma_{in}/i\omega\epsilon_0$, we have, at low frequencies,

using the method outline in the text, Eq.(13)

$$\epsilon_{\text{eff}} \to 3f\frac{\sigma_w}{\omega\epsilon_0}\frac{P''}{a^3} = \frac{9f\sigma_w\left(\sigma_{in}\epsilon'_w - \epsilon'_{in}\sigma_w\right)}{\left(2\sigma_{in}+\sigma_w\right)^2} = 9f\epsilon'_w\frac{\left(\frac{\sigma_{in}}{\sigma_w}-\frac{\epsilon'_{in}}{\epsilon'_w}\right)}{\left(2\frac{\sigma_{in}}{\sigma_w}+1\right)^2} \tag{23}$$

The above equation shows that for any choice of the parameters there is *no* significant enhancement.

For insulating particles (without surface charges) embedded in conducting fluid at low frequencies $P = (\epsilon_{in} - \epsilon_w)/(\epsilon_i + 2\epsilon_w) \to -1/2$ and we recover Maxwell's celebrated result that inserting insulating particles reduces the overall low frequency dielectric constant

$$\epsilon_{eff} = \epsilon_w(1 - \frac{3}{2}f) \tag{24}$$

Appendix II: Planar electrodes

We now briefly contrast our results with those that are known for planar electrodes where the enhancement mars most of the two-electrode dielectric measurements (at low frequency) and makes a four probe measurement essential. The results bear some similarity to the results derived in the text.

The planar electrodes with ideally polarizable interface also shows a dielectric enhancement, not unlike its more well interfacial redox reactions (Faradaic effect) dominated counterpart known as Warburg impedance[29, 30]. The subject of ideally polarized planar electrodes, by itself, is an enormously important problem in electrochemistry [3]. We refer to the skillful and succinct review by Hollingsworth[33–36] and references therein.

For two planar ideally polarized electrodes separated by a distance d, with $\tau = \tau_D(d/2\lambda) = d\lambda/(2D) = \sqrt{\tau_D\tau_L}$; $\tau_L = \frac{(d/2)^2}{D}$. the effective dielectric constant has a canonical Debye form

$$\epsilon'_{eff} = \epsilon'_w\epsilon_0 + \frac{\Delta\epsilon'\,\epsilon_0}{1+i\omega\tau};\;\; \Delta\epsilon' = \epsilon'_w\frac{d}{2\lambda};\;\; \tau = \frac{d\lambda}{2D}, \tag{25}$$

Thus, at low frequencies, $\epsilon'_{eff}(\omega)$, the real part of ϵ_{eff} exceeds the water dielectric constant ϵ'_w by the factor $d/(2\lambda)$. With $\tau_D \sim 10^{-6}$sec and for mm size separation $d/\lambda \sim 10^6$, an enhancement of $\epsilon'_{eff} \sim 10^6\epsilon_w$ can happen for frequencies such that $(d/\lambda)(\omega\tau_D) < 1$ .i.e. $\omega \lesssim 1Hz$.

The results for the planar electrodes are not unlike the results for the sphere: the time constant and enhancements are given by the correspondence $d \leftrightarrow a$, as can be expected from a dimensional analysis[1].

---

[1] A brief account of this work was outlined in J. Qian and P. N. Sen, "Universal dielectric enhancement from externally induced double layer without ζ- potential," (2015), arxiv:1510.06724 [physics.class-ph] .The latter shows near universality of the enhancement and includes many other topics that are not covered in the current paper.

[2] J. Wong. "An electrochemical model of the induced polarization phenomenon in disseminated sulfide ores" Geophysics, 44(7), 1245-1265 (1979)

[3] A. J. Bard and L. R. Faulkner, Electrochemical Methods: Fundamentals and Applications, Wiley, NY (2000)

[4] (1) S. S. Dukhin and V. N. Shilov, Dielectric Phenomena and the Double Layer in Disperse Systems and Polyelectrolytes (Wiley, New York, 1974). Also, Advances in Colloid and Interface Science, (1980) v 13, pp 153 -195 (2) S. S. Dukhin and B. V. Derjaguin, Electrokinetic phenomena. In Surface and Colloid Science; Matijevic, E., Ed.; Wiley: New York, 1974; Vol. 7, 1-351

[5] M. Fixman, J. Chem. Phys., 1983, 78, 1483. M. Fixman, J. Chern. Phys. 72, 5177 (1980); 78,1483 (1983).

[6] W. C. Chew and P. N. Sen, J. Chem. Phys., 1982,77,4683.

[7] E. J. Hinch, J. D. Sherwood, W. C. Chew and P. N. Sen, J. Chem. SOC., Faraday Trans. 2, 1984,80,535-551

[8] E. H. B. DeLacey and L. White, J. Chem. SOC., Furaday Trans. 2, 1981, 77, 2007.;
R. W. O'Brien, Adv. Colloid Interface Sci., 1982, 16, 281;
R. W. O'Brien, J. Colloid Interface Sci., 1983, 92, 13.

[9] H. P. Schwan, G. Schwarz, J. Maczuk , H. J. Pauly, Phys. Chem 66:2626–2635, (1962); H. Pauly and Schwan . Z Naturforsch B 14:125-131(1959)

[10] P. D. Kaviratna , T. Pinnavaia , P. A. Schroeder (1996) J. Phys. Chem Solids, 57(12):1897–1906.

[11] M. Minor, H. van Leeuwen , J. J. Lyklema . Colloid. Interface. Sci, 206:397–406, (1998)

[12] J. C. Maxwell, A Treatise on Electricity and Magnetism (Dover, New York, 1954).

[13] J. C. M. Garnett, Phil. Trans. R. Soc. Lond. 203, 385-420 [1904]

[14] R. Landauer in Electrical transport and optical properties of inhomogeneous media, eds. J. C. Garland and D. B. Tanner, AIP Conf. Proc. No. 40 (1978).

[15] G. K. Batchelor , Annu. Rev. Fluid Mech. 6:227–255, (1974)

[16] M. Bazant and T. Squires Phys. Rev. Lett. 92(6):066101,(2004)

[17] J. Collid and Interface Sci 189, 376?378 (1997)

[18] Murtsovkin V. A., Colloid J. USSR 58, 341-349 (1998)

[19] K Boone, D. Barber and B. Brown (1997) Imaging with electricity, Report of the European Concerted Action on Impedance Tomography, Journal of Medical Engineering and Technology, 21:6, 201-232, D. A. Giljohann, D. S. Seferos, W. L. Daniel, M. D. Massich, P. C. Patel, and C. A. Mirkin, Angewandte Chemie International Edition 49, 3280 (2010); X. Wu, H. Liu, J. Liu, K. N. Haley, J. A. Treadway, J. P. Larson, N. Ge, F. Peale, and M. P. Bruchez, Nature Biotechnology 21, 41 (2003).

[20] P. N. Sen, A. Kleinhammes, Y. Wu, M. Ahmadian-Tehrani (2015) Dielectric Contrast Agents and Methods, US-2015-0167459-A1 , Publication number: 20150167459 Filed: November 24, 2014, Publication date: June 18, 2015. There are other internal patent memos on file with the University of North Carolina, Chapel Hill 27516.

[21] Anderson, B.I., Barber, T.D., L?ling, M.G., Sen, P.N., Taherian, R. and Klein, J., 2008, in 49th Annual Logging Symposium Transactions, Society of Petrophysicists and Well Log Analysts, paper HHHH.

[22] Nelson, P., H., and G. Van Voorhis, Geophysics4,8 , 62-75, 1983; See also André Revil , Gamal Z. Abdel Aal, Estella A. Atekwana, Deqiang Mao , and Nicolas Florsch, **80**, D539-D552, 2015

[23] Levich VG (1962) Physiochemical Hydrodynamics, Prentice-Hall, Englewood Cliffs, NJ.

[24] Wong[2] attributes the data to Collett. L. S., Laboratory investigation of over-voltage. in Over voltage Search and geophysical applications, J. R. Wait, Ed., New YorK, Pergamon Press. 1959 ; See also Grissemann. C., "Examination of the frequency dependent conductivity of ore containing rock on artificial models" Scien. rep. no. 2, Elects . Lab.. Univ. ot Innsbruch, Austria. 1971

[25] Seigel, H., Nabighian, M., Parasnis, D.S., and Vozoff, K., 2007, The Leading Edge, 26, 312-321. See also V. Burtman, H. Fu, M. S. Zhdanov, et al., Geomaterials, 4, 117 (2014)

[26] A. Kleinhammes, and others, Univ. of North Carolina, Unpublished

[27] Curtis, H. J., and Cole, K. S. J. Gen. Physiol., 9.1, 757, 1938; Molinari, R. J. Ph.D. thesis, Brown University, Department of Chemistry, Providence, RI (1977)

[28] M. Wolf, R. Gulich, P. Lunkenheimer, A. Loidl, Biochimica et Biophysica Acta 1810 (2011) 727-740

[29] F. Kohlrausch Pogg. Ann., 148 (1873), p. 143

[30] E. Warburg, Ann. Phys. Chem., 67 (1899), pp. 493-499;

[31] J. D.Ferry, Journal of Chemical Physics, Vol. 16, p.737-739 1948

[32] R. J. Friauf, J. Chem. Phys., 22, 1329, (1954)

[33] H. P. Schwan , Ann Biomed Eng. 20(3) 269-88.(1992); Schwan, H.P. Physical Methods in Biological Research, 4, pp. 323-407. Academic Press, New York, W.L. Nastuk (Ed.) Part B (1963)

[34] J. R. Macdonald,Phys. Rev., 1953, 91,412.; see also, G. Jaffe, Phys. Rev., 1952, 85, 354, H. Chang and G . Jaffe, J . Chem. Phys., 1952,20, 1071, J. R. Macdonald,J. Chem. Phys., 1958, 29, 1346. J. R. Macdonald, Double layer capacitance and relaxation in electrolytes and solids (1970) Transactions of the Faraday Society, 66, pp. 943-958

[35] G. Barbero, and A. L. Alexe-Ionescu, Liquid Crystals, 32 (7), pp. 943-949,(2005)

[36] A. D. Hollingsworth, Current Opinion in Colloid and Interface Science 18, pp 157-159, 2013;